Many-Body Effects in Combined Quantum Mechanical/Molecular Mechanical Simulations of the Hydrated Manganous Ion

Hannes H. Loeffler, Jorge Iglesias Yagüe, and Bernd M. Rode*

Department of Theoretical Chemistry, Institute of General, Inorganic and Theoretical Chemistry, University of Innsbruck, A-6020 Innsbruck, Austria

Received: February 18, 2002; In Final Form: August 3, 2002

Two different quantum mechanics/molecular mechanics molecular dynamics simulation techniques (QM/MM-MD) are compared using as an example the hydrated manganous ion. One includes a perturbation field composed of point charges representing the bulk solvent molecules polarizing the QM region in addition to a quantum chemically derived two-body potential. The other includes the two-body potential plus a three-body correction function. In both simulations, the QM region comprises the ion and its first hydration shell and hence includes all many-body terms up to the QM frontier. The structure of the hydrated ion is discussed in terms of radial distribution functions, coordination numbers, and angular distributions. The results show that both QM/MM-MD techniques agree well with experimental findings for the first-shell hydration structure. QM/MM-MD including point charges has been found to be a satisfactory and economic alternative in studying the first hydration shell without the need to undergo the time-consuming procedure of constructing a three-body correction function from thousands of single-point ab initio computations.

1. Introduction

The implementation of potential functions including three-body or higher-body terms has been found to be mandatory for obtaining correct simulation results for ions in solution, in particular for the structure of the first hydration shell.[1] The construction of higher-body correction terms is a rather complicated and computationally intensive task, especially for systems containing more than two species such as mixed solvents. To overcome these limitations, one can apply the quantum mechanical/molecular mechanical[2−5] (QM/MM) approach, increasing considerably the accuracy of the results. Basically, this methodology divides the total system into two subsystems. One comprises a chemically relevant subsystem calculated at the QM level implicitly including all many-body terms. The other subsystem contains the remaining system calculated at the MM level utilizing an appropriate force field (e.g., one derived from ab initio energy hypersurfaces). This approach has produced very satisfactory results in recent studies on cationic solvation.[6−15] The inclusion of electronic contributions as charge transfer and polarization in the QM region is an essential prerequisite for obtaining correct structural hydration data, especially for transition-metal ions but even for singly charged ions.[15]

Quantum mechanical computations in each step of several thousands in an MD simulation are still very time-consuming and hence the QM region usually has to be restricted to the ion and its nearest neighbors, which in the most minimal case means the first hydration shell. It may still be necessary, however, to include further correction terms because many-body effects may extend to distances larger than the QM region's diameter.[16−18] Thus, the proper description of coupling between QM and MM regions is crucial for the QM/MM approach and in particular for the simulation of ionic systems.

In the present study, two QM/MM-MD simulations were carried out for Mn(II) in water by employing two different combined QM/MM potential approaches. The first one considers the bulk solvent by means of a perturbation field consisting of point charges representing the water molecules at positions taken from the current coordinates in the course of the simulation. The other one includes the same conventional pair potential as in the point-charge simulation and additionally a correction function accounting for explicit three-body effects.

2. Details of Calculations

2.1. QM/MM-MD Methodology. The radius of the quantum mechanical region around the metal ion was set to 4.0 Å in accordance with RDF data from pair-potential-based simulations.[10] Water molecules were allowed to leave and enter from and to this region dynamically. The size of this region contained the full first hydration shell at any step of the simulation. In each simulation step, an ab initio calculation was performed, providing quantum mechanical forces to be incorporated into the total force of the system by[4,19]

$$F(\mathrm{S}) = F_{\mathrm{MM}}(\mathrm{S}) + f_{\mathrm{s}}[F_{\mathrm{QM}}(\mathrm{MM}) - F_{\mathrm{MM}}(\mathrm{MM})] \qquad (1)$$

where $F_{\mathrm{MM}}(\mathrm{S})$ is the MM forces of the total system, $F_{\mathrm{QM}}(\mathrm{MM})$ is the QM forces of the QM region, and $F_{\mathrm{MM}}(\mathrm{MM})$ is the MM forces of the QM region, subtracted to avoid double counting.[5] To ensure a continuous transition of forces between QM and MM regions, a smoothing function f_{s} was applied between 3.8 and 4.0 Å[20]:

$$f_{\mathrm{s}} = 1 \text{ for } r \le r_1$$

$$f_{\mathrm{s}} = \frac{(r_0^2 - r^2)^2(r_0^2 + 2r^2 - 3r_1^2)}{(r_0^2 - r_1^2)^3} \text{ for } r_1 < r \le r_0 \qquad (2)$$

$$f_{\mathrm{s}} = 0 \text{ for } r > r_0$$

---

* Corresponding author. E-mail: bernd.m.rode@uibk.ac.at.

10.1021/jp020443k CCC: $22.00

where r_1 and r_0 define the lower and upper bounds, respectively, of the smoothing region.

The simulations were carried out with the QM/MM-MD software developed in our department[20] using the parallelized TURBOMOLE[21,22] package, version 5.1 for the calculation of the ab initio forces and the inclusion of the surrounding point charges into the Hamiltonian. The basis sets used were the relativistic compact effective potentials (RCEP) and double-ζ valence basis set developed by Stevens et al.[23] for the Mn(II) ion and Dunning's DZP[24,25] for oxygen and DZ[24,25] for hydrogen. The same basis sets had been employed in the construction of the pair potential and three-body correction.[10,26] All computations were performed on two dual Intel Pentium III 550-MHz machines working in parallel and using a standard 100 Mbit Ethernet interlink. The total computation times were about 7 months (point charges) and 9 months (2+3-body), respectively.

2.2. QM/MM-MD Simulation Including Point Charges. Water molecules located farther away than 4.0 Å from the ion were included in the Hamiltonian as a set of point charges of -0.6597 for oxygens and $+0.3298$ for hydrogens in accordance with the CF2 water model.[27] The location of the point charges was determined by the respective positions of the water molecules in the course of the simulation. The system consisted of 1 Mn(II) and 199 water molecules in a periodic cube at a temperature of 298.16 K. A radial cutoff limit of half the box length (9.12 Å) for Coulombic and non-Coulombic terms was chosen, with the exception of non-Coulombic O−H and H−H interactions, where cutoffs of 5.0 and 3.0 Å, respectively, were sufficient. A reaction field[28,29] was established to account for long-range Coulombic interactions properly. The density of 0.997 g cm^{-3} was assumed to be the same as that of pure water. Because CF2 water is a flexible model, the integration time step was set to 0.2 fs. Only a two-body potential was used for the MM region.[10] The system was equilibrated for 4.6 ps in a canonical *NVT* ensemble, with a starting configuration from a previous classical pair potential only MD simulation.[26] The data for structural evaluation was collected from another 4.0 ps of simulation.

2.3. QM/MM-MD Simulation Including a Three-Body Correction Term. The simulation protocol was basically the same as in the previous section with the following exceptions: the system consisted of 1 Mn(II) and 499 water molecules in a periodic cube. The radial cutoff limit was set to half the box length (12.35 Å), and the system was equilibrated for 4.1 ps. The data for structural evaluation was sampled within another 11.6 ps.

The classical potential function was combined from two-body interactions and a three-body correction function (2+3-body) that has been described in detail elsewhere.[13,26] Briefly, the construction involves the generation of the H_2O−Mn−H_2O energy hypersurface under the assumption of dipole orientation of the water molecules where the Mn−H_2O distances and H_2O−Mn−H_2O angles are varied between 1.5 and 6.0 Å and 180−60°. The hypersurface is then fitted to

$$E_{3bd}^{corr} = A_1 \exp(-A_2 r_{12}) \exp(-A_2 r_{13}) \exp(-A_3 r_{23}) \times (r_{limit} - r_{12})^2 (r_{limit} - r_{13})^2 \qquad (3)$$

where A_1, A_2, and A_3 are fitting parameters that are found to be 0.7138 kcal mol^{-1}, 0.2857 Å^{-1}, and 0.5313 Å^{-1}, respectively;[26] r_{12}, r_{13}, and r_{23} are the distances between Mn−O and O−O; and r_{limit} is a cutoff limit (set to 6.0 Å) up to which the three-body corrections are evaluated. The last two quadratic terms ensure a smooth approach to zero for both energies and forces.

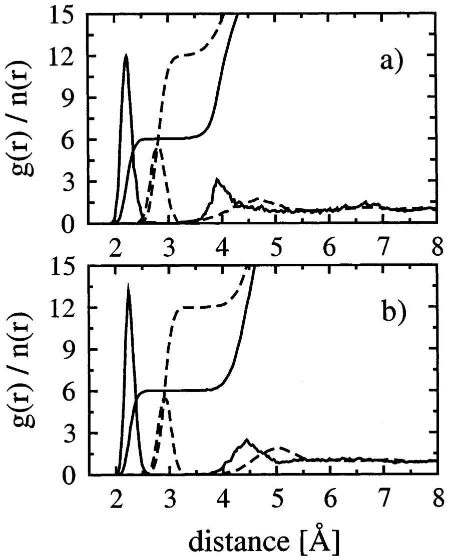

Figure 1. Radial distribution functions Mn−O (−) and Mn−H (− − −) obtained from a point-charge simulation (a) and a 2+3-body simulation (b).

TABLE 1: Characteristic Values of the Mn−O RDF Obtained from Various Simulations and Experimental Values[a]

method	r_{M_1}	r_{m_1}	n_1	r_{M_2}	r_{m_2}	n_2	reference
QM/MM point charges	2.23	2.81	6.00	3.91	5.85	18.31	this work
QM/MM 2+3-body	2.25	2.85	6.00	4.45	5.07	14.47	this work
QM/MM 2-body	2.28	2.88	6.74	4.00	5.20	18.06	10
classical 2+3-body	2.35	3.41	6.08	4.77	5.53	21.25	26
classical 2-body	2.22	3.26	8.74	4.42	5.62	22.74	10
experiment	2.18[b]/2.20[c]		6				30−32

[a] Distances r_{M_i} and r_{m_i} (Å) denote the *i*th maximum and minimum of the RDF, respectively, and n_i is the average coordination number integrated up to r_{m_i} of the *i*th shell. [b] EXAFS: 1 M $Mn(ClO_4)_2$, ref 30 [c] X-ray scattering: 2.2 M $Mn(ClO_4)_2$, ref 31; 0.6, 1.1, and 2.8 M $MnSO_4$, ref 32.

3. Results and Discussion

The Mn−O and Mn−H radial distribution functions (RDF) with their corresponding integration numbers for both the point charge and 2+3-body simulation are plotted in Figure 1.

The general picture is that of a first hydration shell well-separated from the second shell, where the intershell region is practically zero over a range of about 1 Å. Furthermore, the first peak is very sharp, suggesting a rather rigid first hydration shell structure.

The characteristic values of the RDFs are summarized in Table 1 together with results from experiments[30−33] and previous calculations.[10,26]

The peaks corresponding to the first hydration shell of the Mn−O RDF are located at distances of 2.23 Å in the point-charge simulation and 2.25 Å in the 2+3-body simulation. The second-shell peaks, however, are quite different in both simulations. In the point-charge simulation, the maximum is located at 3.9 Å whereas that of the 2+3-body simulation is located at 4.5 Å. The different box sizes of the two simulations are certainly not responsible for this behavior. Classical MD simulations with a single Mn ion in 199 and 499 water molecules revealed first and second hydration shell peaks of

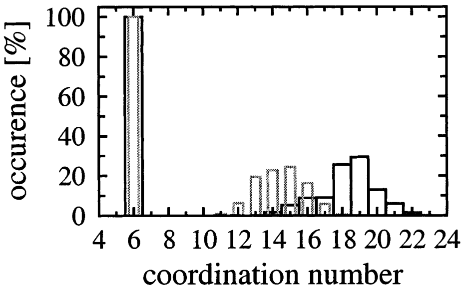

Figure 2. Coordination-number distributions of first and second hydration shells obtained from a point-charge simulation (black bars) and a 2+3-body simulation (grey bars).

the same heights and positions. The only difference was found at distances larger than 6.0 Å, where the 199 water box tends to overemphasize the structure and yields spurious peaks. This does not seem too surprising given the smaller box size and cutoff radius. Therefore, the larger distance of the second-shell maximum of the 2+3-body simulation must be attributed to the purely repulsive nature of the three-body corrections (eq 3). This function has been constructed mainly with the first shell in mind and has not been explicitly parametrized for first-shell−second-shell interactions.

The data in Table 1 demonstrates that the inclusion of at least three-body corrections is absolutely necessary to reproduce correct first-shell coordination numbers in accordance with experiment.[30−33] Pure classical two-body potentials are much too attractive, and even QM/MM-MD simulations have difficulties if the QM−MM coupling fails to describe the interactions between QM and MM properly.[15] The first-shell peak maxima are close to the experimental results except in the case of the classical 2+3-body simulation because of the repulsive three-body correction (eq 3). The QM/MM-MD 2+3-body simulation, in contrast, reproduces these distances quite well.

The experimental values have been obtained from $MnSO_4$ and $Mn(ClO_4)_2$ solutions of 1 to 2.8 M and range from 2.18 to 2.20 Å.[30−33] However, these distances are not directly comparable with our results because of the rather high concentration and thus the inevitable counterion effect. Furthermore, the second shell is difficult to detect experimentally, and no generally applicable method exists.[34] The EXAFS study,[30,33] for instance, assumes the structure beyond the first hydration shell to be that of bulk water. Thermodynamic data is virtually absent for the transition-metal ion Mn^{2+}, although the Gibbs free energy of hydration has been reported.[35] However, various approximations and assumptions have to be made to separate the counterion contribution from the ion under investigation.[36]

Figure 2 shows the coordination-number distributions of the first and second hydration shells.

The coordination numbers of the first shell calculated from the integrations up to the first minimum of the RDF yield 100% hexacoordination for the manganous ion in both simulations, in full agreement with the experimental findings.[33] The mean coordination numbers of the second hydration shells are 18.3 and 14.5 for the point charge and 2+3-body simulation, respectively. That means that every water molecule of the first shell is coordinated to 3.1 and 2.4 water molecules, on average, of the second shell. The coordination number of the point-charge simulation is close to 19.3 obtained from a classical 2+3-body MD simulation.[26] Although differing substantially in quality, all simulations lead to the same conclusion: interactions between first- and second-shell ligands are not solely determined by hydrogen bonding.

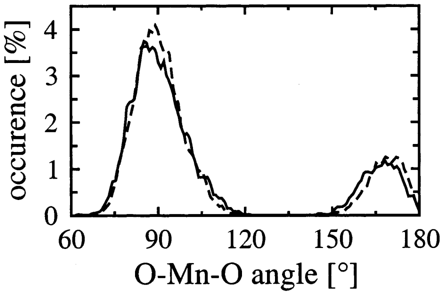

Figure 3. O−Mn−O angular distribution functions of the first shell obtained from a point-charge simulation (—) and a 2+3-body simulation (− − −).

Figure 3 depicts the $H_2O-Mn-H_2O$ angular distribution functions.

The peak maxima are located at 85 and 168° in the point-charge simulation and at 89 and 172° in the 2+3-body simulation. Hence, both simulations predict a very similar structure of a nearly regular octahedron. The two peaks are clearly separated from each other, indicating low angular flexibility of the water ligands in the first hydration sphere. Supporting this notion, both peaks are rather narrow with angle populations of just 80−100° and 160−175° at peak half-height.

4. Summary and Conclusions

The results of both the point-charge and 2+3-body simulations (Table 1) have shown that high-quality potentials are crucial to the reliable reproduction of experimental findings. Experimental difficulties make it necessary to perform such simulations in order to elucidate in more detail the hydration structure of electrolyte solutions. Furthermore, we have shown in recent studies of Cu^{2+} [9] and Ni^{2+},[13] both ions having been extensively investigated experimentally,[33] that our QM/MM-MD approach is a valuable tool in predicting the hydration structure of transition-metal ions in accordance with experiments.

The explicit inclusion of the polarization of the QM region by means of point charges does not show any significant differences compared to the 2+3-body simulation. Both point-charge and 2+3-body simulations describe the first shell equally well. Assuming the first-row transition metals have a well-defined second hydration shell, the 2+3-body simulation seems to be the better alternative. However, the purely repulsive description of the three-body corrections casts some doubt on the quality of the second-shell peak. Increasing the diameter of the QM region would clarify this issue, but computation times are expected to increase strongly, and care should be taken to describe the now important water−water interactions properly.

Acknowledgment. Financial support by the Austrian Science Foundation, project no. P13644-TPH, is gratefully acknowledged.

References and Notes

(1) Elrod, M. J.; Saykally, R. J. *Chem. Rev.* **1994**, *94*, 1975.

(2) Gao, J. In *Reviews in Computational Chemistry*; Lipkowitz, K. B., Boyd, D. B., Eds.; VCH Publishers: New York, 1996; Vol. 7

(3) Bakowies, D.; Thiel, W. *J. Phys. Chem.* **1996**, *100*, 10580.

(4) Maseras, F. *Chem. Commun.* **2000**, *25*, 1821.

(5) Sherwood, P. Hybrid Quantum Mechanics/Molecular Mechanics Approaches. In *Modern Methods and Algorithms of Quantum Chemistry*; Grotendorst, J., Ed.; NIC Series (http://www.fz-juelich.de/nic-series/): Jülich, Germany, 2000; Vol. 3.

(6) Kerdcharoen, T.; Rode, B. M. *J. Phys. Chem. A* **2000**, *104*, 7073.

(7) Tongraar, A.; Rode, B. M. *J. Phys. Chem. A* **2001**, *105*, 506.

(8) Tongraar, A.; Sagarik, K.; Rode, B. M. *J. Phys. Chem. B* **2001**, *105*, 10559.

(9) Marini, G. W.; Liedl, K. R.; Rode, B. M. *J. Phys. Chem. A* **1999**, *103*, 11387.

(10) Yagüe, J. I.; Mohammed, A. M.; Loeffler, H.; Rode, B. M. *J. Phys. Chem. A* **2001**, *105*, 7646.

(11) Schwenk, C. F.; Loeffler, H. H.; Rode, B. M. *J. Chem. Phys.* **2001**, *115*, 10808.

(12) Schwenk, C. F.; Loeffler, H. H.; Rode, B. M. *Chem. Phys. Lett.* **2001**, *349*, 99.

(13) Inada, Y.; Mohammed, A. M.; Loeffler, H. H.; Rode, B. M. *J. Phys. Chem. A* **2002**, *106*, 6783.

(14) Inada, Y.; Loeffler, H. H.; Rode, B. M. *Chem. Phys. Lett.* **2002**, *358*, 449.

(15) Loeffler, H. H.; Rode, B. M. *J. Chem. Phys.* **2002**, *117*, 110.

(16) Clementi, E.; Kistenmacher, H.; Kolos, W.; Romano, S. *Theor. Chim. Acta* **1980**, *55*, 257.

(17) Ortega-Blake, I.; Novaro, O.; Leś, A.; Rybak, S. *J. Chem. Phys.* **1982**, *76*, 5405.

(18) Ortega-Blake, I.; Hernández, J.; Novaro, O. *J. Chem. Phys.* **1984**, *81*, 1894.

(19) Svensson, M.; Humbel, S.; Froese, R. D. J.; Matsubara, T.; Sieber, S.; Morokuma, K. *J. Phys. Chem.* **1996**, *100*, 19357.

(20) Kerdcharoen, T.; Liedl, K. R.; Rode, B. M. *Chem. Phys.* **1996**, *211*, 313.

(21) Ahlrichs, R.; von Arnim, M. In *Methods and Techniques in Computational Chemistry: METECC-95*; Clementi, E., Corongiu, G., Eds.; STEF: Cagliari, 1995.

(22) Ahlrichs, R.; Elliott, S. D.; Huniar, U. *Ber. Bunsen-Ges. Phys. Chem.* **1998**, *102*, 795.

(23) Stevens, W. J.; Krauss, M.; Basch, H.; Jasien, P. G. *Can. J. Chem.* **1992**, *70*, 612.

(24) Dunning, T. H., Jr. *J. Chem. Phys.* **1989**, *90*, 1007.

(25) Dunning, T. H., Jr.; Hay, P. J. In *Modern Theoretical Chemistry: Methods of Electronic Structure Theory;* Schaeffer, H. F., III, Ed.; Plenum Press: New York, 1977; Vol. 3.

(26) Yagüe, J. I.; Mohammed, A. M.; Loeffler, H.; Rode, B. M. *J. Mol. Struct.: THEOCHEM*, in press.

(27) Stillinger, F. H.; Rahman, A. *J. Chem. Phys.* **1978**, *68*, 666.

(28) van Gunsteren, W. F.; Berendsen, H. J. C.; Rullman, J. A. C. *Faraday Discuss. Chem. Soc.* **1978**, *66*, 58.

(29) Adams, D. J.; Adams, E. M.; Hills, G. J. *Mol. Phys.* **1979**, *38*, 387.

(30) Sham, T. K.; Hastings, J. B.; Perlman, M. L. *Chem. Phys. Lett.* **1981**, *83*, 391.

(31) Ohtaki, H.; Yamaguchi, T.; Maeda, M. *Bull. Chem. Soc. Jpn.* **1976**, *49*, 701.

(32) Shapovalov, I. M.; Radchenko, I. V. *J. Struct. Chem.* **1971**, *12*, 705.

(33) Othaki, H.; Radnai, T. *Chem. Rev.* **1993**, *93*, 1157.

(34) Ohtaki, H. *Chem. Mon.* **2001**, *132*, 1237.

(35) Marcus, Y. *J. Chem. Soc., Faraday Trans.* **1991**, *87*, 2995.

(36) Marcus, Y. *Pure Appl. Chem.* **1987**, *59*, 1093.